Electronic Supplementary Material (ESI) for Inorganic Chemistry Frontiers.

Supporting Information

Unraveling the effect of carbon morphology evolution in hard carbons on sodium storage performance

Huilan Sun[a], Qiaoyan Zhang[a], Fei Yuan[a], Di Zhang[a], Zhaojin Li[a], Qiujun Wang[a], Huan Wang[a,], Bo Wang[a,]**

[a] *Hebei Key Laboratory of Flexible Functionals Materials, School of Materials Science and Engineering, Hebei University of Science and Technology, Shijiazhuang 050000, PR China.*

Email: wangbo1996@gmail.com (B. Wang), wanghuantp@163.com (H. Wang)

** Corresponding author.*

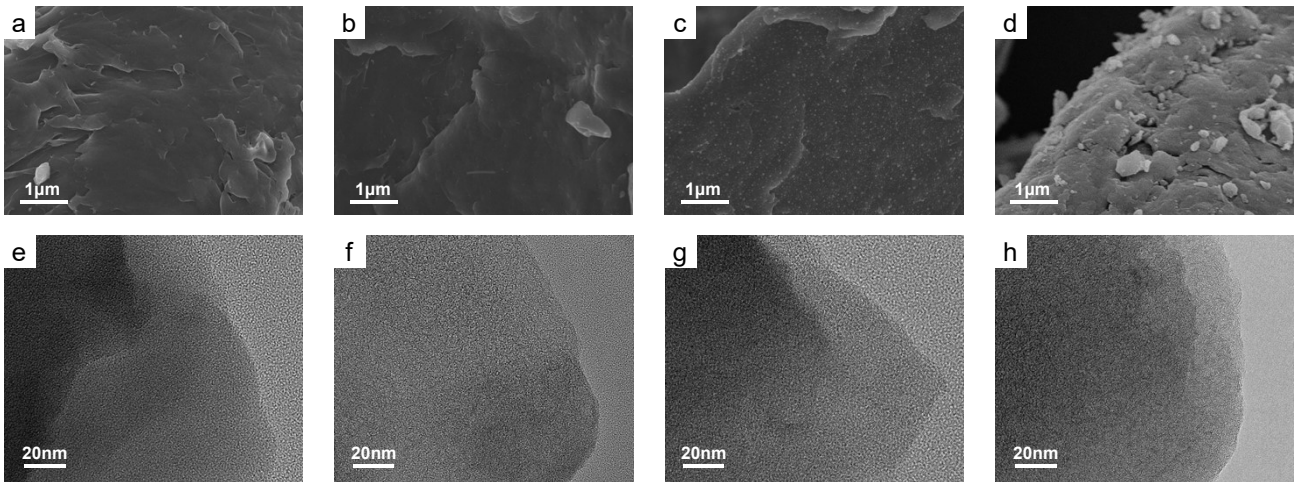

Fig. S1 SEM and TEM images of CHC-T, (a, e) CHC-700, (b, f) CHC-1100, (c, g) CHC-1300 and (d, h) CHC-1500.

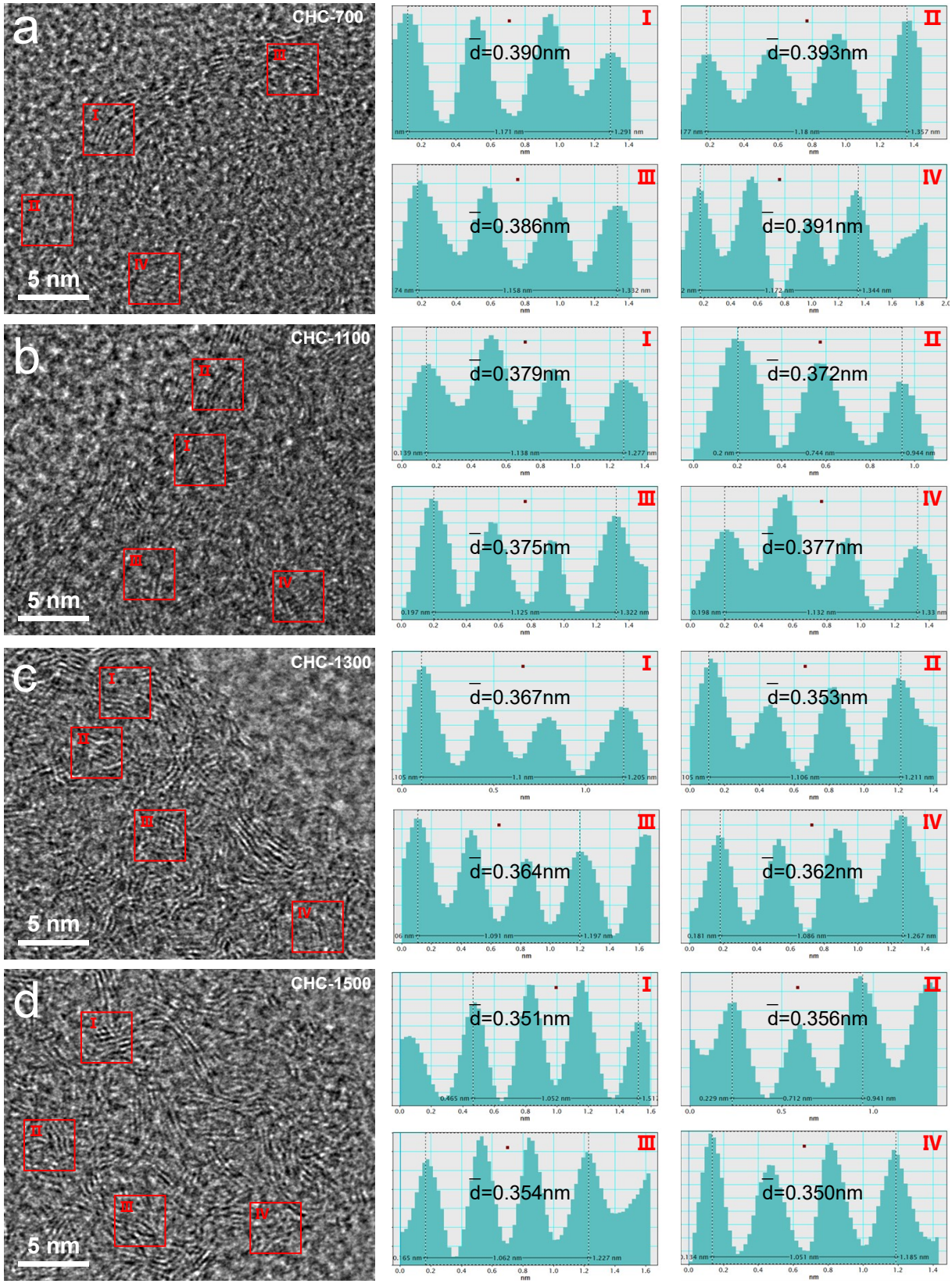

Fig. S2 Interlayer distance of CHC-T, (a) CHC-700, (b) CHC-1100, (c) CHC-1300 and (d) CHC-1500.

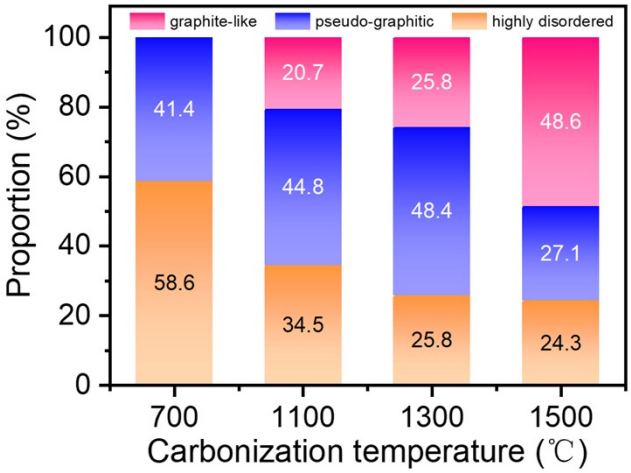

Fig. S3 The proportion of highly disordered domains, pseudo-graphitic domains and graphite-like domains for CHC-T.

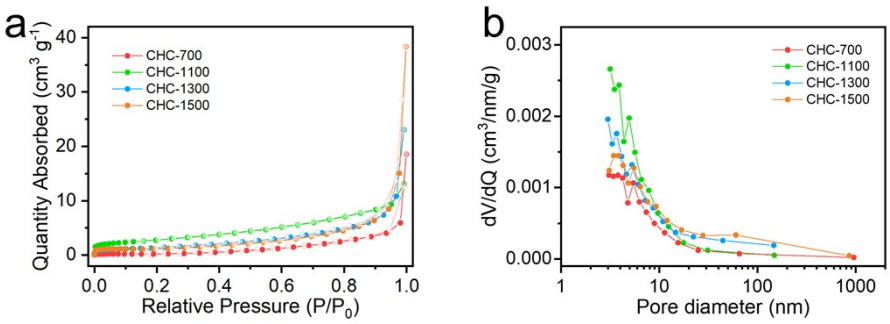

Fig. S4 (a) N_2 adsorption–desorption isotherms, (b) pore size distribution curves.

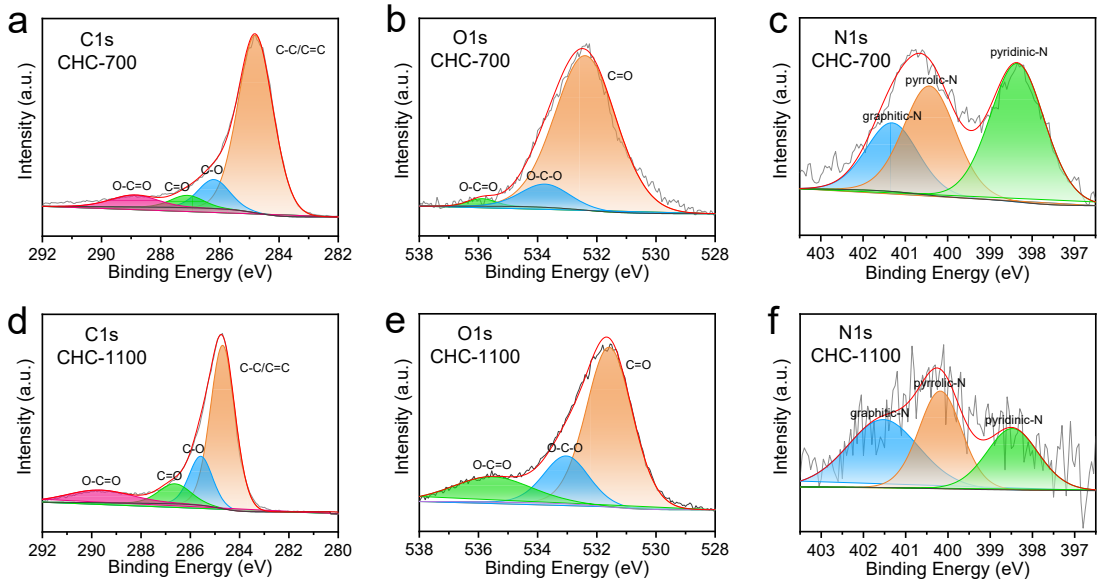

Fig. S5 High-resolution C 1s, O 1s and N 1s XPS spectra of (a-c) CHC-700 and (d-f) CHC-1100.

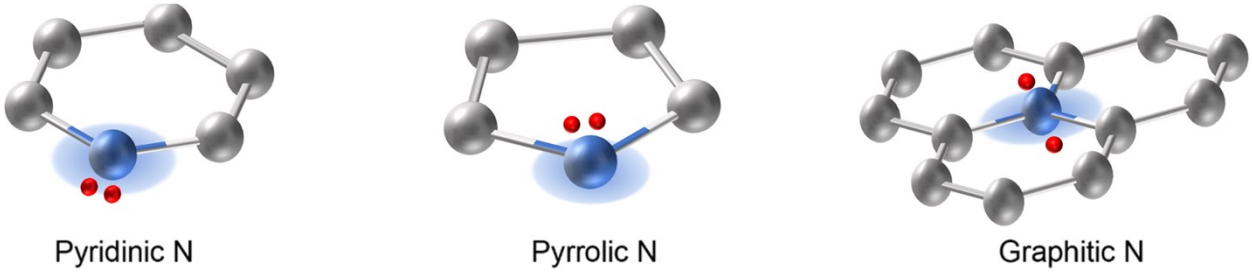

Fig. S6 Electron configurations for pyridinic N, pyrrolic N, and graphitic N.

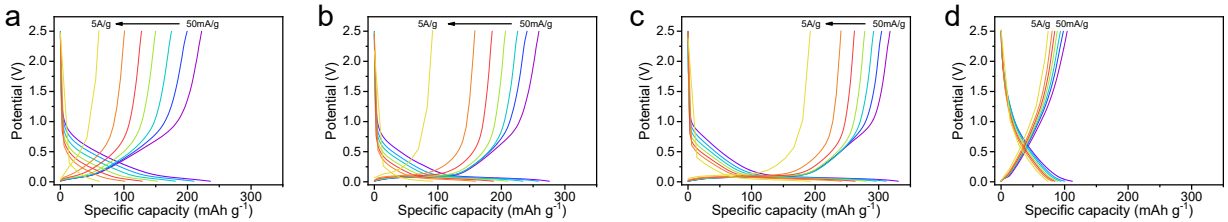

Fig. S7 Rate performance images of (a) CHC-700, (b) CHC-1100, (c) CHC-1300 and (d) CHC-1500.

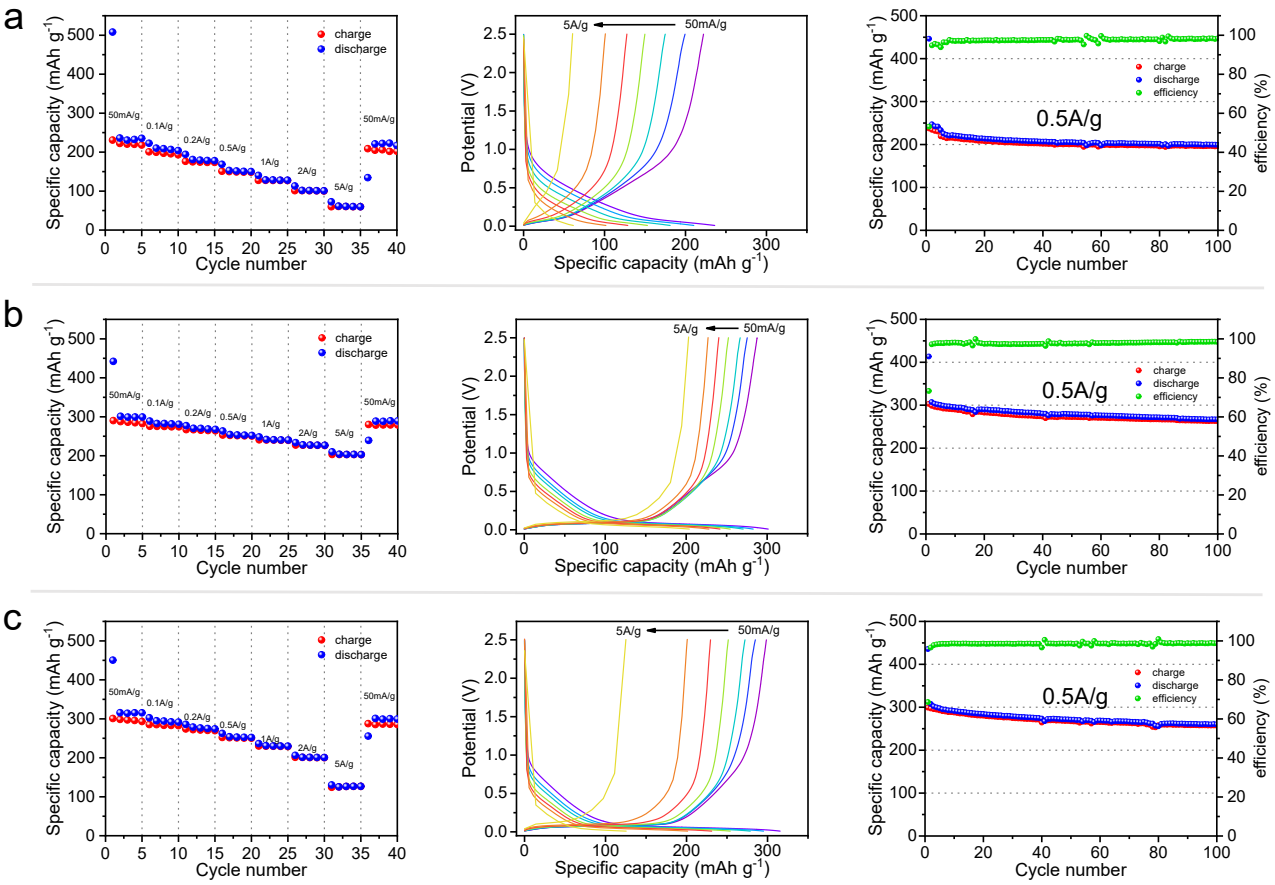

Fig. S8 Electrochemical performance images of (a) CHC-900, (b) CHC-1200 and (c) CHC-1400.

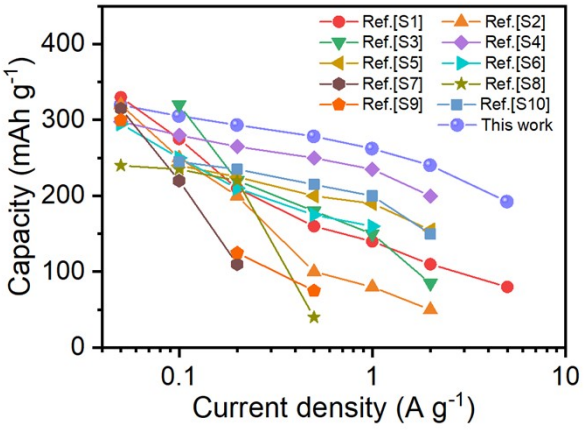

Fig. S9 Comparison of rate capability between CHC-1300 and ever reported carbon anode materials in literatures.

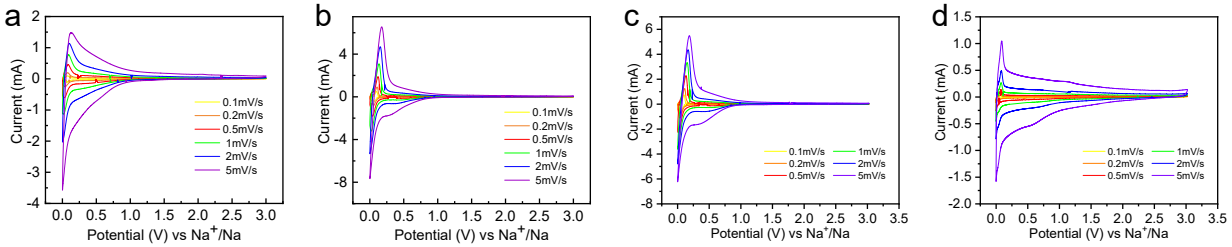

Fig. S10 CV curves at different scan rates, (a) CHC-700, (b) CHC-1100, (c) CHC-1300 and (d) CHC-1500.

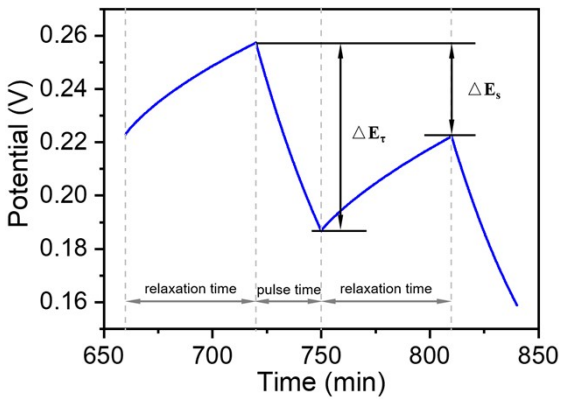

Fig. S11 *E vs. t* profile for one GITT test. D_{Na+} was predicted by the following equation:

$$D = \frac{4}{\pi\tau}\left(\frac{n_m V_m}{s}\right)^2\left(\frac{\triangle E_s}{\triangle E_\tau}\right)^2$$

Where n_m is the amount of active substance of electrode material, V_m is the molar volume, and S represents geometric area. $\triangle E_s$ and $\triangle E_\tau$ can be obtained from the GITT curves.

Table S1. Physical parameters of CHC-T from XRD

Sample	2θ (°)	$\bar{d}_{(002)}$ (nm)	L_a (nm)	L_c (nm)
CHC-700	22.9	0.388	1.86	1.03
CHC-1100	23.6	0.376	2.33	1.09
CHC-1300	24.3	0.365	2.84	1.14
CHC-1500	25.1	0.355	3.02	1.21

Table S2. Specific surface area and pore diameter of CHC-T from BET

Sample	S_{BET} (m^2 g^{-1})	$\bar{d}_{pore}$ (nm)
CHC-700	0.928	3.08
CHC-1100	9.068	3.17
CHC-1300	4.729	3.00
CHC-1500	4.490	3.44

References

1 N. Sun, Z. Guan, Y. Liu, Y. Cao, Q. Zhu, H. Liu, Z. Wang, P. Zhang and B. Xu, Extended "Adsorption–Insertion" Model: A New Insight into the Sodium Storage Mechanism of Hard Carbons, *Adv. Energy Mater.*, 2019, **9**, 1901351.

2 S. Alvin, C. Chandra and J. Kim, Controlling intercalation sites of hard carbon for enhancing Na and K storage performance, *Chem. Eng. J.*, 2021, **411**, 128490.

3 D. Cheng, X. Zhou, H. Hu, Z. Li, J. Chen, L. Miao, X. Ye and H. Zhang, Electrochemical storage mechanism of sodium in carbon materials: A study from soft carbon to hard carbon, *Carbon N. Y.*, 2021, **182**, 758–769.

4 R. Guo, C. Lv, W. Xu, J. Sun, Y. Zhu, X. Yang, J. Li, J. Sun, L. Zhang and D. Yang, Effect of

Intrinsic Defects of Carbon Materials on the Sodium Storage Performance, *Adv. Energy Mater.*, 2020, **10**, 1903652.

5 C. Xu, W. Yang, G. Ma, S. Che, Y. Li, Y. Jia, N. Chen, G. Huang and Y. Li, Edge-Nitrogen Enriched Porous Carbon Nanosheets Anodes with Enlarged Interlayer Distance for Fast Charging Sodium-Ion Batteries, *Small*, 2022, **18**, 2204375.

6 F. Sun, H. Wang, Z. Qu, K. Wang, L. Wang, J. Gao, J. Gao, S. Liu and Y. Lu, Carboxyl-Dominant Oxygen Rich Carbon for Improved Sodium Ion Storage: Synergistic Enhancement of Adsorption and Intercalation Mechanisms, *Adv. Energy Mater.*, 2021, **11**, 2002981.

7 B. X. Ran Xu，Ning Sun, Huanyu Zhou, Xiaqing Chang, Razium A. Soomro, Hard carbon anodes derived from phenolic resin/sucrose cross - linking network for high-performance sodium - ion batteries, *Batter. Energy*, 2022, **2**, 20220054.

8 X. Liu, X. Jiang, Z. Zeng, X. Ai, H. Yang, F. Zhong, Y. Xia and Y. Cao, High Capacity and Cycle-Stable Hard Carbon Anode for Non flammable Sodium-Ion Batteries, *ACS Appl. Mater. Interfaces*, 2018, **10**, 38141–38150.

9 X. Zhang, X. Dong, X. Qiu, Y. Cao, C. Wang, Y. Wang and Y. Xia, Extended low-voltage plateau capacity of hard carbon spheres anode for sodium ion batteries, *J. Power Sources*, 2020, **476**, 228550.

10 Y. W. Yu Liu, Haodong Dai, Yongkang An, Lijun Fu, Qinyou An, A Facile and Scalable Synthesis of Sulfur, Selenium and Nitrogen co-doped Hard Carbon Anode for High Performance Na- and K-ion Batteries, *J. Mater. Chem. A*, 2020, **8**, 14993–15001.